International Scholarly Research Network
ISRN Condensed Matter Physics
Volume 2012, Article ID 950354, 6 pages
doi:10.5402/2012/950354

Research Article

Photoluminescence of Zinc Oxide Nanowires: The Effect of Surface Band Bending

Dake Wang and Nicholas Reynolds

Department of Physics, Furman University, Greenville, SC 29613, USA

Correspondence should be addressed to Dake Wang, dake.wang@furman.edu

Received 4 January 2012; Accepted 29 January 2012

Academic Editors: J. Brault, H. Hibino, and V. Kochereshko

The photoluminescence of zinc oxide nanowires was investigated via the thermal annealing treatment in oxygen-rich and oxygen-poor conditions. Dramatic changes in the relative intensity of the ultraviolet and the green visible luminescence were observed following different annealing treatments. The changes in photoluminescence bear little correlation to the changes in the oxygen-to-zinc ratios that were revealed using Raman scattering and other characterization techniques. The chemisorption of oxygen and the subsequent surface band bending, instead of the oxygen vacancy concentration, are shown to be the mechanism that determines the observed changes in photoluminescence.

1. Introduction

The luminescence of zinc oxide (ZnO) exhibits a band edge ultraviolet (UV) emission peak related to the exciton luminescence and a broad green luminescence (GL) band related to deep level defects. ZnO has a very large exciton binding energy of 60 meV, almost three times that of the gallium nitride [1], giving it a unique place in the family of the wide-bandgap semiconductors. This large exciton binding energy allows the free exciton luminescence to be readily observed at room temperature and to persist at a temperature as high as 700 K [2]. The relationship between the UV and the green luminescence often becomes more complicated in ZnO nanostructures, where surface effects, owning to the very large surface-to-volume ratio, introduce additional factors to affect the photoluminescence (PL) processes.

The mechanism of the defect-related electron-hole recombination process and the identity of the defect state has been the subject of extensive research effort. However, no consensus has been reached and the topic remains controversial. Among the different defects proposed to explain the visible luminescence, oxygen vacancies (V_o) have been widely considered as the most likely candidate [3–6]. Oxygen annealing was usually employed to modify the level of oxygen deficiency in ZnO. However, contradictory results regarding the effect of annealing on the luminescence property of ZnO have been reported. In some experiments [7–9], oxygen annealing has enhanced the intensity of the visible luminescence band and has reduced the intensity of the band edge UV luminescence band, while in some other experiments, the exact opposite trend was observed [10, 11]. It was also found that the change in relative intensities of the visible and UV luminescence band depends on the annealing temperature [12, 13]. The different growth methods and postgrowth treatments result in different surface conditions, and the concentration and spatial distribution of native or foreign defects also vary among samples. When comparing such PL data, caution needs to be exercised since all these factors can contribute to the characteristics of PL.

In this work, thermal annealing in oxygen-rich and oxygen-poor conditions was employed to investigate the defect states and the mechanism governing the green luminescence in ZnO nanowires. The oxygen-to-zinc ratio was barely modified by the oxygen annealing and decreased by the vacuum annealing. The relative intensity of the green luminescence band increased significantly after the oxygen annealing and decreased after the vacuum annealing. This result is inconsistent with the assumption that a higher level of oxygen deficiency (in forms of V_o) gives rise to a higher

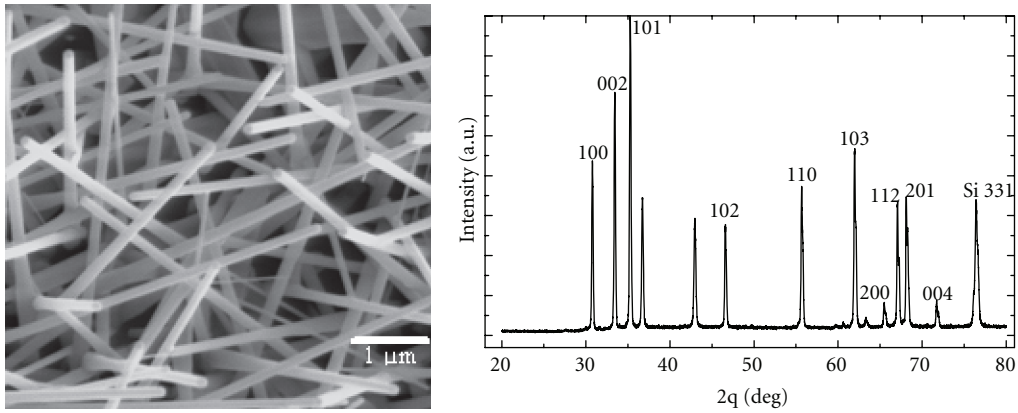

(a) (b)

Figure 1: (a) SEM of as-grown ZnO nanowires. (b) XRD of as-grown ZnO nanowires.

concentration of recombination centers for GL; however, can be elucidated by taking the effect of surface band bending into consideration.

2. Experiment

The ZnO nanowires were grown on Si(100) substrates at 550°C using a thermal chemical vapor deposition system. The zinc powder (99.998%, Aldrich) was placed in an alumina boat located inside the quartz tube reactor. The growth took about 45 minutes under 25 Torr of a mixture of argon and oxygen gas with a flow rate of 125 sccm and 20 sccm, respectively. A more detailed description of the sample preparation can be found in [14].

The as-grown ZnO nanowire sample was cut into two pieces, one of which was annealed in an oxidation furnace purged with flowing oxygen gas at 800°C for 1 hr, while the other one was annealed in vacuum at 800°C for 1 hr.

Room temperature PL spectra were collected immediately before or after the annealing treatments using a Jobin-Yvon spectrometer and the 325 nm (20 mW) line of a He-Cd laser (Kimmon Electric). All PL spectra were collected under the same experimental conditions. An objective lens was used to deliver the laser light to the sample, as well as to collect the PL light from the sample. The size of the laser spot on the sample is about 20 μm in diameter.

3. Results and Discussion

3.1. Material Characterizations and Stoichiometric Analysis. Prior to the annealing treatments, the morphology and crystallization of the as-grown sample were characterized by using scanning electron micrograph (SEM) and X-ray diffraction (XRD). Figure 1(a) shows that the majority of the nanowires have a diameter of between 100 nm and 200 nm and a length of several micrometers. The morphological and size distribution of the nanowires was found to be fairly uniform across the samples. The XRD pattern confirms the wurtzite lattice structure and the random orientation of the nanowires. The fact that the FWHMs of the diffraction peaks are smaller than 0.2° indicates that nanowires consist of high-quality crystals.

Table 1: The E_2-to-LO Raman intensity ratios and the UV-to-GL PL intensity ratios collected before the annealing treatments (as-grown) and after the annealing treatments.

	As-grown	Oxygen annealing	Vacuum annealing
E_2/1st LO	4.3	4.2	3.6
E_2/2nd LO	0.23	0.22	0.18
UV/GL	0.4	0.023	0.9

Raman spectra of the as-grown sample are shown in Figure 2. All the Raman active modes are observed due to the random orientation of the nanowires. The sharp E_2 mode peak at around 440 cm^{-1} is an indication of long phonon lifetime and high crystal quality, and the mixing of A_1(LO) and E_1(LO) gives rise to the LO peak at around 580 cm^{-1}.

Raman spectra were also collected after the annealing treatments. The integrated intensities of the E_2, the 1st-order LO, and the 2nd-order LO modes were determined from the Raman spectra, and the intensity ratios of E_2-to-LO modes are listed in Table 1.

The E_2-to-LO intensity ratio has been shown to increase with increasing oxygen-to-zinc ratio in ZnO: a consequence of the decrease of the defect states introduced by the excess zinc [15, 16]. Table 1 shows that the oxygen-to-zinc ratio of the sample annealed in oxygen-rich condition was nearly the same as that of the as-grown sample, and the oxygen-to-zinc ratio of the sample annealed in oxygen-poor condition was reduced. Auger electron spectroscopy was also performed, and similar conclusion regarding the oxygen-to-zinc ratios was obtained. The reason that the oxygen annealing failed to increase the oxygen-to-zinc ratio was probably due to the insufficient oxygen pressure in the annealing furnace.

In order to rule out the possibility of any microstructure change such as coalescence, recrystallization, and grain growth, which may occur during the annealing treatments, SEM and XRD were performed after the annealing

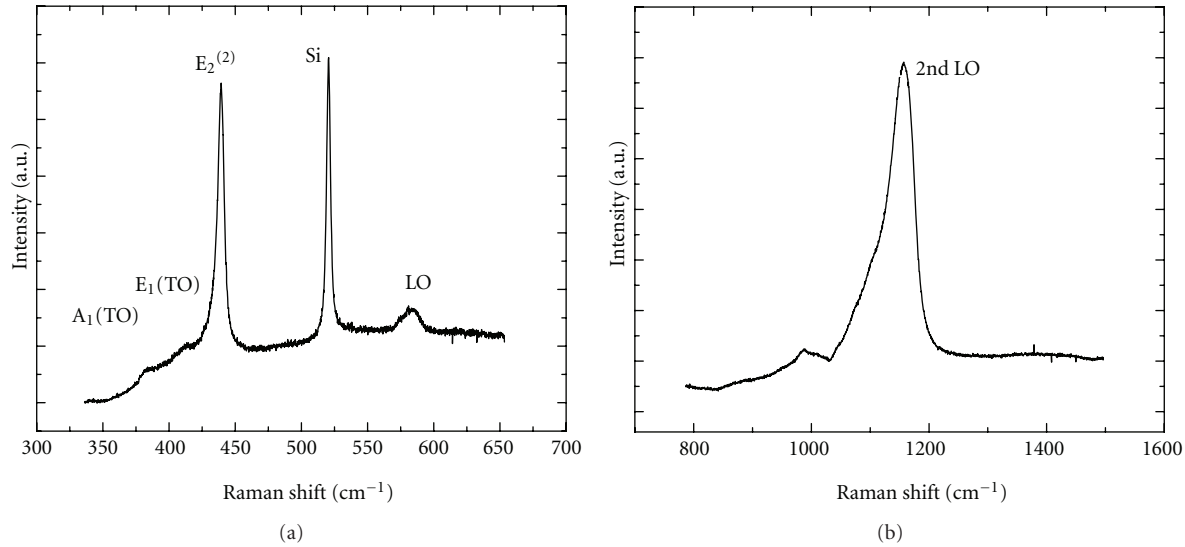

Figure 2: Raman spectrum of the as-grown ZnO nanowires showing (a) the 1st-order modes and (b) the 2nd-order modes.

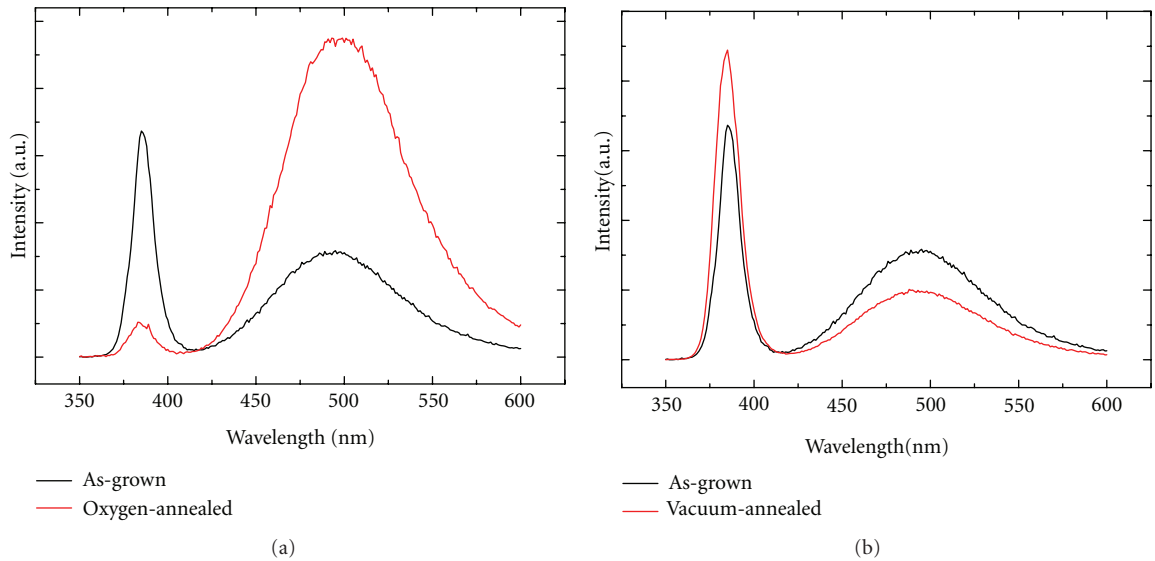

Figure 3: Room temperature PL spectra collected before and after (a) the oxygen annealing and (b) the vacuum annealing. The PL spectra collected before the annealing treatments are plotted in black.

treatments. Neither SEM nor XRD showed any major change when compared to those obtained for the as-grown sample.

3.2. Photoluminescence and Surface Band Bending. Figure 3 shows the PL spectra collected before and after the annealing treatments. All PL spectra are characterized by a UV and a broad GL band located at about 3.2 eV and 2.5 eV, respectively, and no other obvious visible luminescence bands could be identified. The oxygen annealing led to significant increase in the GL at the expense of the UV luminescence. The vacuum annealing led to increase in UV luminescence at the expense of the GL. The integrated intensities of the UV and the GL bands were determined from the PL spectra, and the intensity ratios of UV-to-GL, before and after the annealing treatments, are listed in Table 1.

As revealed by the stoichiometric analysis (see Table 1), the level of oxygen deficiency did not experience any significant change after the oxygen annealing. Therefore, the change in V_o concentration can be safely dismissed as the main cause of the dramatic reduction in the UV-to-GL intensity ratio (from 0.4 to 0.023) observed after the oxygen annealing. The change in the PL spectra after the vacuum annealing poses as an even greater puzzle: despite an increasing level of oxygen deficiency after the vacuum annealing, the UV-to-GL intensity ratio increased (from 0.4 to 0.9) rather than decreased.

We believe that the apparent contradiction can be largely explained by the change in the level of chemisorption of oxygen at the surface after different annealing treatments. It is well known that the chemisorption of oxygen at the ZnO surface causes an upward band bending by capturing electrons in regions near the surface [5, 6, 17]. This adsorption can occur in the air at room temperature, producing an upward band bending and a surface depletion region in the as-grown ZnO. Upon excitation, the photo-generated electrons and holes near the surface are swept to the opposite directions across the depletion region, thus reducing their chances of recombination through excitonic processes. Indeed, it has been found that surface passivation by coating ZnO thin film or nanostructures with surfactant [18], alkali halide [19], or a dielectric layer [20] can reduce the band bending, thus suppressing GL and enhancing UV luminescence.

The depth of the surface recombination layer was estimated to be 30 nm [21]. Muth et al. have found a large absorption coefficient of ~160,000 cm^{-1} at 325 nm, which corresponds to a penetration depth of ~60 nm [22]. Since a substantial number of photo-generated electrohole pairs fall within the surface depletion region, any change of the depletion layer will have a significant impact on the overall characteristics of luminescence.

Lagowski et al. have found that the 0.72 eV thermal activation energy needed for the charge transfer through the surface potential barrier is the major limiting factor for determining the chemisorption rate. They have also found that the rate of charge transfer increases linearly with increasing oxygen pressure and exponentially with increasing temperature [17]. In our experiment, annealing at an elevated temperature in oxygen ambient greatly increased the number of chemisorbed oxygen species, leading to the enhanced GL. On the other hand, vacuum annealing partially removed the preexisting chemisorbed oxygen at the surface of the as-grown sample, leading to the enhanced UV luminescence.

In addition to the dissociation of the photo-generated electron-hole pairs, the surface band bending also facilitates the ionization of V_o. This latter mechanism worked in unison with the dissociation mechanism to achieve the observed changes in PL.

Based on the growth method and the result of the stoichiometric analysis, it should be expected that our ZnO samples are oxygen deficient and are populated with asubstantial number of V_o. The charged states (singly ionized V_o^+, doubly ionized V_o^{++}, or neutral V_o^0) of V_o depend on the energetic location of the Fermi level. We have previously determined the free carrier concentration for ZnO nanowires to be $n = 3.76 \times 10^{17}\ cm^{-3}$ [23]. The energetic location of the Fermi level can then be calculated using the equation [24] $n = N_c \exp(-(E_c - E_f)/k_B T)$, where $N_c = (2/h^3)(2\pi\ m^* k_B T)^{3/2}$, h and k_B are Planck's and Boltzmann's constants, and E_c and E_f are the energies of the conduction band edge and Fermi level, respectively. Using the effective mass of the electron in ZnO for m^* and the room temperature for T, the Fermi level is found to be ~50 meV below the conduction band edge.

Because the Fermi level is close to the conduction band edge in our samples, it should stay above the levels of both neutral and singly ionized V_o in the flat-band region beyond the depletion layer. Consequently, V_o should exist in its neutral state in the flat-band region [25]. The first principle calculations have also shown that the neutral state is energetically favored if the Fermi level is close to the conduction band edge [26]. With sufficient extent of band bending, the Fermi level will lie between the levels of neutral and singly ionized V_o in the depletion region (see Figure 4(a)), and V_o should exist in its singly ionized state [3, 4, 25]. Therefore, in our samples, the depletion region is populated with V_o^+, while the interior of the nanowires is populated with V_o^0. Given V_o^+ as the recombination center of GL [3–6, 25, 27], GL should be spatially localized near the surface of the nanowires in our samples. Indeed, both the comparative study of nanowires with different surface to volume ratios [28] and the direct imaging using cathodoluminescence microscopy [29] have shown that the GL process is localized near the surface of the nanowires.

The effects of the surface band bending on the UV luminescence and GL processes are summarized in Figure 4. During the oxygen annealing, the extent of band bending increased and the depletion region grew in size, causing more photo-generated electron-hole pairs to dissociate. At the same time, an increasing number of V_o were ionized into V_o^+ which were localized in the depletion region. The free holes swept into the depletion region then recombined with the electrons occupying V_o^+ to generate GL. The UV luminescence was suppressed and was pushed further into the interior of the nanowires. The opposite processes that occurred during the vacuum annealing enhanced the UV luminescence, suppressed the GL, and pushed it further out to the surface (see Figure 4(c)). Note that the recombination of an electron occupying V_o^+ with a free hole implies that the energetic level of V_o^+ is at ~2.5 eV above the valence band, which is consistent with the ~0.7 eV shift of the absorption edge observed in ZnO samples annealed in oxygen-poor conditions [30].

The charged state of V_o and their distributions in ZnO nanostructures depend on the energetic location of the Fermi level and the extent of band bending, as well as the size of the nanostructures. In case of a low free carrier concentration, the Fermi level may lie between the levels of V_o and V_o^+ in the flat-band region [3, 4]. Consequently, the GL is localized in the interior, and a greater extent of band bending will suppress the GL rather than enhance it, which is exactly the opposite of what was observed in our experiment. In case of very small or highly porous ceramics, the depletion regions may occupy the entire structure, that is, it is depleted through, and all the V_o may be ionized into V_o^+ or V_o^{++} [27].

4. Conclusion

In summary, the oxygen-to-zinc ratio was barely modified by the oxygen annealing, and it was reduced by the vacuum annealing. The relative intensity of GL was greatly increased after the oxygen annealing, and it was reduced after the vacuum annealing. There was no simple correlation between

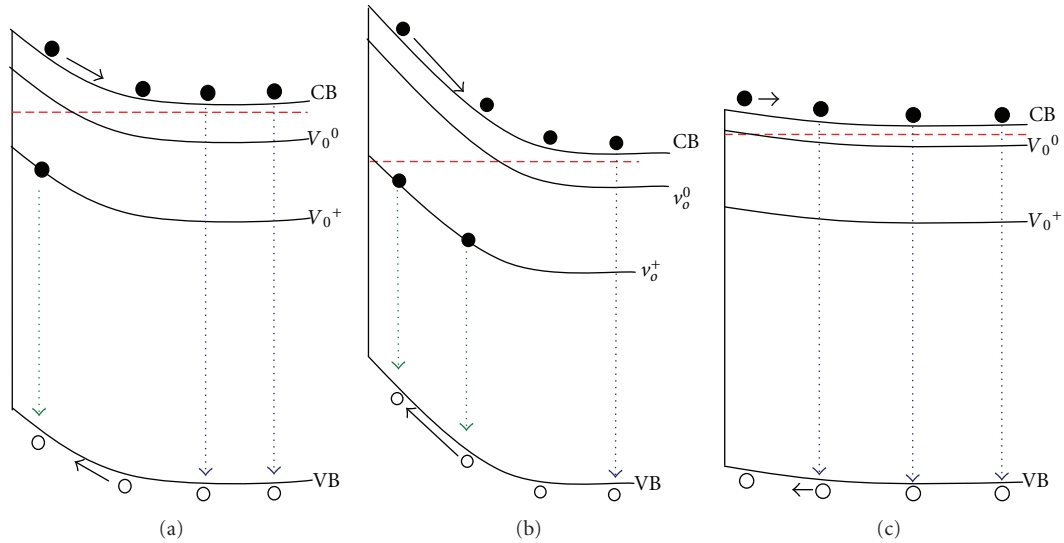

Figure 4: Schematics of the energy band diagram (not to scale) for (a) as-grown, (b) oxygen annealed, and (c) after vacuum annealed samples, illustrating the band bending and charged states of V_o near the surface. Solid dots are electrons and empty circles are holes. The vertical dotted lines depict the radiative recombination processes, where GL is plotted in green and the UV luminescence in blue. The Fermi level is the red dashed line. The dissociation of the electron-hole pairs is indicated with arrows.

the level of the oxygen deficiency and the changes in the PL spectra observed after the annealing treatments. The increase in the relative intensity of GL after the oxygen annealing can be explained by the greater extent of the chemisorption of oxygen and the subsequent surface band bending. The surface band bending affects the PL processes primarily via two mechanisms: the dissociation of the photogenerated electron-hole pairs and the creation of V_o^+ in the depletion region, both of which enhance the GL at the expense of UV luminescence. The vacuum annealing affected the chemisorption of oxygen and the surface band bending in the opposite fashion.

Acknowledgments

The authors would like to thank the Research and Professional Growth Committee at Furman University for partial support through the RPG Grant. Portions of the work were also supported by Furman University through the Furman Advantage Research Fellowship.

References

[1] O. Madelung, U. Rössler, and M. Schulz, Eds., *Gallium Nitride (GaN), Enery gap, Exciton Binding Energy*, The LB Volumes III/17A-22A-41A1b, SpringerMaterials—The Landolt-Börnstein Database, 2002.

[2] X. B. Chen, J. Huso, J. L. Morrison, and L. Bergman, "The properties of ZnO photoluminescence at and above room temperature," *Journal of Applied Physics*, vol. 102, no. 11, Article ID 116105, 2007.

[3] K. Vanheusden, W. L. Warren, C. H. Seager, D. R. Tallant, J. A. Voigt, and B. E. Gnade, "Mechanisms behind green photoluminescence in ZnO phosphor powders," *Journal of Applied Physics*, vol. 79, no. 10, pp. 7983–7990, 1996.

[4] K. Vanheusden, C. H. Seager, W. L. Warren, D. R. Tallant, and J. A. Voigt, "Correlation between photoluminescence and oxygen vacancies in ZnO phosphors," *Applied Physics Letters*, vol. 68, no. 3, pp. 403–405, 1996.

[5] A. Van Dijken, E. A. Meulenkamp, D. Vanmaekelbergh, and A. Meijerink, "The kinetics of the radiative and nonradiative processes in nanocrystalline ZnO particles upon photoexcitation," *Journal of Physical Chemistry B*, vol. 104, no. 8, pp. 1715–1723, 2000.

[6] A. Van Dijken, E. A. Meulenkamp, D. Vanmaekelbergh, and A. Meijerink, "Identification of the transition responsible for the visible emission in ZnO using quantum size effects," *Journal of Luminescence*, vol. 90, no. 3, pp. 123–128, 2000.

[7] T. Sekiguchi, N. Ohashi, and Y. Terada, "Effect of hydrogenation on ZnO luminescence," *Japanese Journal of Applied Physics Part 2*, vol. 36, no. 3, pp. L289–L291, 1997.

[8] X. Liu, X. Wu, H. Cao, and R. P. H. Chang, "Growth mechanism and properties of ZnO nanorods synthesized by plasma-enhanced chemical vapor deposition," *Journal of Applied Physics*, vol. 95, no. 6, pp. 3141–3147, 2004.

[9] W. S. Shi, O. Agyeman, and C. N. Xu, "Enhancement of the light emissions from zinc oxide films by controlling the post-treatment ambient," *Journal of Applied Physics*, vol. 91, no. 9, p. 5640, 2002.

[10] B. Lin, Z. Fu, Y. Jia, and G. Liao, "Defect photoluminescence of undoping ZnO films and its dependence on annealing conditions," *Journal of the Electrochemical Society*, vol. 148, no. 3, pp. G110–G113, 2001.

[11] M. Anpo and Y. Kubokawa, "Photoluminescence of zinc oxide powder as a probe of electron-hole surface processes," *Journal of Physical Chemistry*, vol. 88, no. 23, pp. 5556–5560, 1984.

[12] S. H. Bae, S. Y. Lee, H. Y. Kim, and S. Im, "Effects of post-annealing treatment on the light emission properties of ZnO thin films on Si," *Optical Materials*, vol. 17, no. 1-2, pp. 327–330, 2001.

[13] Y. G. Wang, S. P. Lau, H. W. Lee et al., "Photoluminescence study of ZnO films prepared by thermal oxidation of Zn

metallic films in air," *Journal of Applied Physics*, vol. 94, no. 1, pp. 354–358, 2003.

[14] A. J. Cheng, Y. Tzeng, Y. Zhou et al., "Thermal chemical vapor deposition growth of zinc oxide nanostructures for dye-sensitized solar cell fabrication," *Applied Physics Letters*, vol. 92, no. 9, Article ID 092113, 2008.

[15] M. Tzolov, N. Tzenov, D. Dimova-Malinovska et al., "Vibrational properties and structure of undoped and Al-doped ZnO films deposited by RF magnetron sputtering," *Thin Solid Films*, vol. 379, no. 1-2, pp. 28–36, 2000.

[16] G. J. Exarhos and S. K. Sharma, "Influence of processing variables on the structure and properties of ZnO films," *Thin Solid Films*, vol. 270, no. 1-2, pp. 27–32, 1995.

[17] J. Lagowski, E. S. Sproles, and H. C. Gatos, "Quantitative study of the charge transfer in chemisorption; Oxygen chemisorption on ZnO," *Journal of Applied Physics*, vol. 48, no. 8, pp. 3566–3575, 1977.

[18] D. Li, Y. H. Leung, A. B. Djurišić et al., "Different origins of visible luminescence in ZnO nanostructures fabricated by the chemical and evaporation methods," *Applied Physics Letters*, vol. 85, no. 9, pp. 1601–1603, 2004.

[19] Y. Harada and S. Hashimoto, "Enhancement of band-edge photoluminescence of bulk ZnO single crystals coated with alkali halide," *Physical Review B*, vol. 68, no. 4, Article ID 045421, 4 pages, 2003.

[20] K. C. Hui, H. C. Ong, P. F. Lee, and J. Y. Dai, "Effects of AlOx-cap layer on the luminescence and photoconductivity of ZnO thin films," *Applied Physics Letters*, vol. 86, no. 15, Article ID 152116, pp. 1–3, 2005.

[21] Y. G. Wang, S. P. Lau, H. W. Lee et al., "Photoluminescence study of ZnO films prepared by thermal oxidation of Zn metallic films in air," *Journal of Applied Physics*, vol. 94, no. 1, pp. 354–358, 2003.

[22] J. F. Muth, R. M. Kolbas, A. K. Sharma, S. Oktyabrsky, and J. Narayan, "Excitonic structure and absorption coefficient measurements of ZnO single crystal epitaxial films deposited by pulsed laser deposition," *Journal of Applied Physics*, vol. 85, no. 11, pp. 7884–7887, 1999.

[23] A. J. Cheng, Y. Tzeng, H. Xu et al., "Raman analysis of longitudinal optical phonon-plasmon coupled modes of aligned ZnO nanorods," *Journal of Applied Physics*, vol. 105, no. 7, Article ID 073104, 2009.

[24] M. P. Marder, *Condensed Matter Physics*, John-Wiley, New York, NY, USA, 2000.

[25] S. A. Studenikin and M. Cocivera, "Time-resolved luminescence and photoconductivity of polycrystalline ZnO films," *Journal of Applied Physics*, vol. 91, no. 8, p. 5060, 2002.

[26] A. Janotti and C. G. Van De Walle, "Oxygen vacancies in ZnO," *Applied Physics Letters*, vol. 87, no. 12, Article ID 122102, pp. 1–3, 2005.

[27] K. Bouzid, A. Djelloul, N. Bouzid, and J. Bougdira, "Electrical resistivity and photoluminescence of zinc oxide films prepared by ultrasonic spray pyrolysis," *Physica Status Solidi A*, vol. 206, no. 1, pp. 106–115, 2009.

[28] I. Shalish, H. Temkin, and V. Narayanamurti, "Size-dependent surface luminescence in ZnO nanowires," *Physical Review B*, vol. 69, no. 24, Article ID 245401, 2004.

[29] T. Nobis, E. M. Kaidashev, A. Rahm, M. Lorenz, J. Lenzner, and M. Grundmann, "Spatially inhomogeneous impurity distribution in ZnO micropillars," *Nano Letters*, vol. 4, no. 5, pp. 797–800, 2004.

[30] F. A. Selim, M. H. Weber, D. Solodovnikov, and K. G. Lynn, "Nature of native defects in ZnO," *Physical Review Letters*, vol. 99, no. 8, Article ID 085502, 2007.